Geomechanics and Engineering, *Vol. 5, No. 5 (2013) 419-445*
DOI: http://dx.doi.org/10.12989/gae.2013.5.5.419

Undrained strength-deformation characteristics of Bangkok Clay under general stress condition

Siam Yimsiri [1], Wanwarang Ratananikom [1],
Fumihiko Fukuda [2] and Suched Likitlersuang[*3]

[1] *Department of Civil Engineering, Faculty of Engineering, Burapha University, Chonburi, Thailand*
[2] *Faculty of Engineering, Hokkaido University, Sapporo, Hokkaido, Japan*
[3] *Department of Civil Engineering, Faculty of Engineering, Chulalongkorn University, Bangkok, Thailand*

(Received January 16, 2012, Revised May 06, 2013, Accepted May 16, 2013)

Abstract. This paper presents an experimental study on the influence of principal stress direction and magnitude of intermediate principal stress on the undrained stress-strain-strength behaviors of Bangkok Clay. The results of torsional shear hollow cylinder and advanced triaxial tests with various principal stress directions and magnitudes of intermediate principal stress on undisturbed Bangkok Clay specimens are presented. The analysis of testing results include: (i) stress-strain and pore pressure behaviors, (ii) stiffness characteristics, and (iii) strength characteristics. The results assert clear evidences of anisotropic characteristics of Bangkok Clay at pre-failure and failure conditions. The magnitude of intermediate principal stress for plane-strain condition is also investigated. Both failure surface and plastic potential in deviatoric plane of Bangkok Clay are demonstrated to be isotropic and of circular shape which implies an associated flow rule. It is also observed that the shape of failure surface in deviatoric plane changes its size, while retaining its circular shape, with the change in direction of major principal stress. Concerning the behavior of Bangkok Clay found from this study, the discussions on the effects of employed constitutive modeling approach on the resulting numerical analysis are made.

Keywords: torsional shear hollow cylinder; stress-strain characteristics; failure criteria; generalised stress; Bangkok Clay

1. Introduction

Natural soils are believed to possess cross-anisotropic behavior due to their mode of deposition which is one-dimensional in nature. Anisotropic consolidation stresses align platety particles and particle groups with their long axes perpendicular to the major principal stress. As a result, the mechanical behavior of natural soils will depend on changes in the orientations and magnitudes of the principal stresses which are common situations of most geotechnical constructions. These effects should be investigated to better understand the fundamental behavior of soil which is necessary for the development of advanced constitutive models so that the formulated stress-strain characteristics can be used for reliable prediction of soil behavior in the field. Such developments are primarily based on experimental data from laboratory tests.

*Corresponding author, DPhil., E-mail: suched.l@eng.chula.ac.th

http://www.techno-press.org/?journal=gae&subpage=7 ISSN: 2005-307X (Print), 2092-6219 (Online)

The conventional triaxial apparatus (TX) has been commonly used in the laboratory. It offers only two stress states which are the non-continuous change of the major principal stress direction (α) between 0° in compression and 90° in extension modes coupled with a jump of the intermediate principal stress parameter (b) from 0 to 1. To evaluate the behavior of soil element under more realistic and general loading conditions, it is desirable to be able to control the magnitudes and directions of all three principal stresses independently. The plane strain (PS) apparatus and directional shear cell (DSC) offer attractive capabilities for examining of anisotropic characteristics; however, they cannot control b. True triaxial (TTX) and torsional shear hollow cylinder (TSHC) are the most popular apparatuses to study soil behavior under general stress condition. The TSHC apparatus is capable of: (i) achieving acceptable uniform distributions of the stresses, (ii) fully independent controls over and measurement of stresses σ_z, σ_r, σ_θ, $\tau_{z\theta}$, and (iii) accurate measurement of strains ε_z, ε_r, ε_θ, $\gamma_{z\theta}$. The TSHC apparatus is the only laboratory test which can control both major principal stress direction and magnitude of intermediate principal stress.

Anisotropic characteristics of undisturbed clay under general stress condition have been widely studied by TTX (e.g., Kuwano and Bhattarai 1989, Kirkgard and Lade 1991, 1993, Callisto and Calabresi 1998 and Callisto and Rampello 2002) but with much lesser data by TSHC (e.g., Gasparre *et al*. 2007, Nishimura *et al*. 2007). Among TSHC data available, there are very limited data on TSHC with independent control of α and b. In addition, despite its common field occurrence, very little research has been conducted to study the response of Bangkok Clay under general stress condition. Therefore, there is lack of data for Bangkok Clay to facilitate its formulation of advanced constitutive model which considers the effects of major principal stress direction and magnitude of intermediate principal stress into account.

Presented here is an experimental study of the undrained deformation and strength characteristics of Bangkok Clay under general stress condition. The TSHC and triaxial tests are performed on undisturbed Bangkok Clay specimens under undrained compression/extension condition (CIUC/E) with various principal stress directions and magnitudes of intermediate principal stress. To the best of the Authors' knowledge, this research is the first instance for Bangkok Clay where such combined loading response has been systematically investigated with explicit accounting for the variation of principal stress rotations and magnitudes of intermediate principal stress on an individual basis.

2. Description of experimental program

The essential features of the TSHC system used in this study were described by Fukuda *et al*. (1997). The apparatus was stress-controlled by a computer-based closed-loop servo-system. The hollow cylindrical specimens had inner diameter = 30 mm, outer diameter = 70 mm, and height = 120 mm. Fig. 1 shows three normal stresses which are axial (σ_z), radial (σ_r), circumferential (σ_θ), and one shear stress ($\tau_{\theta z}$) components on the soil element in TSHC. These stresses can be controlled by adjusting torque (M_T), axial force (W), outer cell pressure (p_o), and inner cell pressure (p_i). Fig. 1 also shows the work-conjugate strain components ε_z, ε_r, ε_θ, and $\gamma_{z\theta}$. In this study, the average stress and strain components on soil element were calculated according to the equations given by Hight *et al*. (1983). The inclination of major principal stress with respect to in-situ vertical direction (α) and the magnitude of intermediate principal stress which is usually represented in term of b parameter are defined in Eqs. (1) and (2), respectively.

$$\alpha = \frac{1}{2}\tan^{-1}\left(\frac{2\tau_{\theta z}}{\sigma_z - \sigma_\theta}\right) \tag{1}$$

$$b = \frac{\sigma_2 - \sigma_3}{\sigma_1 - \sigma_3} \tag{2}$$

All TSHC specimens were isotropically consolidated to their in-situ mean effective stresses before undrained sheared at constant mean total stress (constant p). The in-situ effective stresses were calculated from unit weights profiles, groundwater pressure profile considering drawdown condition (Phien-Wej *et al*. 2006), and coefficient of earth pressure at rest (K_o) from pressuremeter tests (Prust *et al*. 2005). A back pressure of 200 kPa was applied to ensure specimen saturation. After completion of the saturation process, the Skempton B parameter was greater than 0.95. The termination of the isotropic consolidation stage was judged from the dissipation of the excess pore

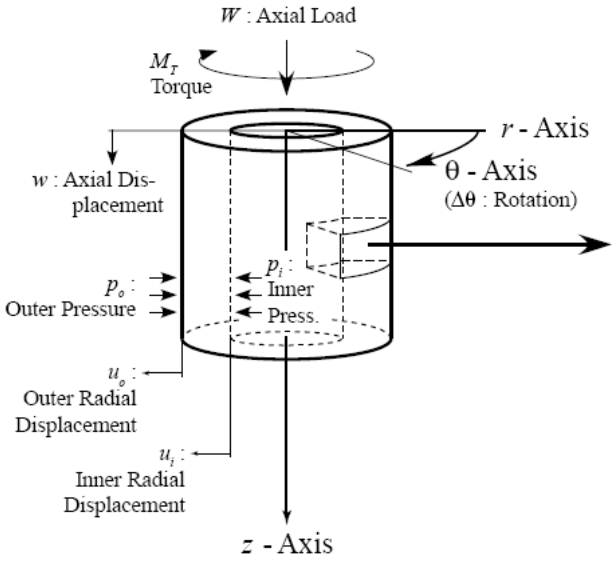

(a) TSHC specimen

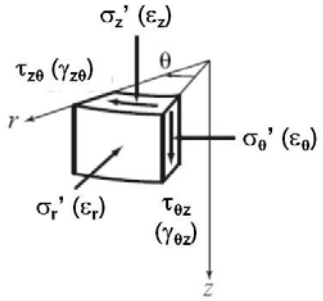

(b) Stresses and strains

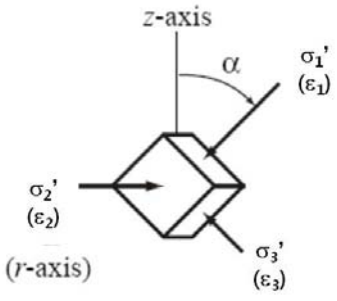

(c) Principal stresses and strains

Fig. 1 Stress and strain components within TSHC specimen (Zdravkovic and Jardine 2000)

pressure (Δu < 1 kPa). In case of compression and extension mode, specimens were sheared until achieving failure at large strain. However, in case of tests with $\alpha = 45°$, the final shearing stage was terminated when either failure was observed or the angle of rotation exceeded 30°. The loading speed of shearing stage was prescribed by the rate of increase in principal stress ratio ($d(\sigma_1'/\sigma_3')/dt$) of 0.00075/min which was sufficient to ensure fully equalized pore pressure.

The advanced triaxial apparatus, incorporated with local axial and radial strain measurement systems, was also employed in this study, the detail of which was described by Yimsiri *et al.* (2009). Submersible LVDTs (Cuccovillo and Coop 1997) were used for local axial strain measurement and proximity transducers (Hird and Yung 1989) were used for local radial strain measurement. The TX specimens had diameter of 50 mm and height typically of 100 mm. The specimens were also isotropically consolidated to their in-situ mean effective stresses before subjected to standard undrained compression shearing which involved axial loading under strain-controlled condition, with nominal external axial strain rate of 0.2%/hr, while keeping the cell pressure constant. In this study, the TX data supplement TSHC data in that: (i) TX data provide additional data where TSHC data may be less reliable due to stress-nonuniformity and (ii) TX data can investigate small-strain behavior.

The undisturbed Bangkok Clay specimens were retrieved from the ground by ϕ 100 mm piston sampler from Lad Prao area in Bangkok between the depths of 7.0-14.6 m. The profiles of soil properties are presented in Fig. 2 together with locations of all specimens. Most of the soil specimens were taken from medium clay stratum with index properties of approximately: Liquid Limit (LL) ≈ 54-88%, Plastic Limit (PL) ≈ 18-33%, Plasticity Index (PI) ≈ 35-58%, natural water content (w_n) ≈ 23-55%, and total unit weight (γ) ≈ 17.0 kN/m^3. The OCRs of all specimens are between 1.2-1.5 (Shibuya *et al.* 2001). Nine torsional shear tests were carried out each with different α and b values. The α values were fixed at 0°, 45°, and 90° and the b values were fixed at 0, 0.5, and 1. The torsional shear hollow cylinder test program is shown in Table 1. The symbols A and B stand for α and b, respectively, and the numbers afterward indicate their values (e.g., A00B05 means $\alpha = 0°$ and $b = 0.5$). The triaxial test program is shown in Table 2. The CIUC tests

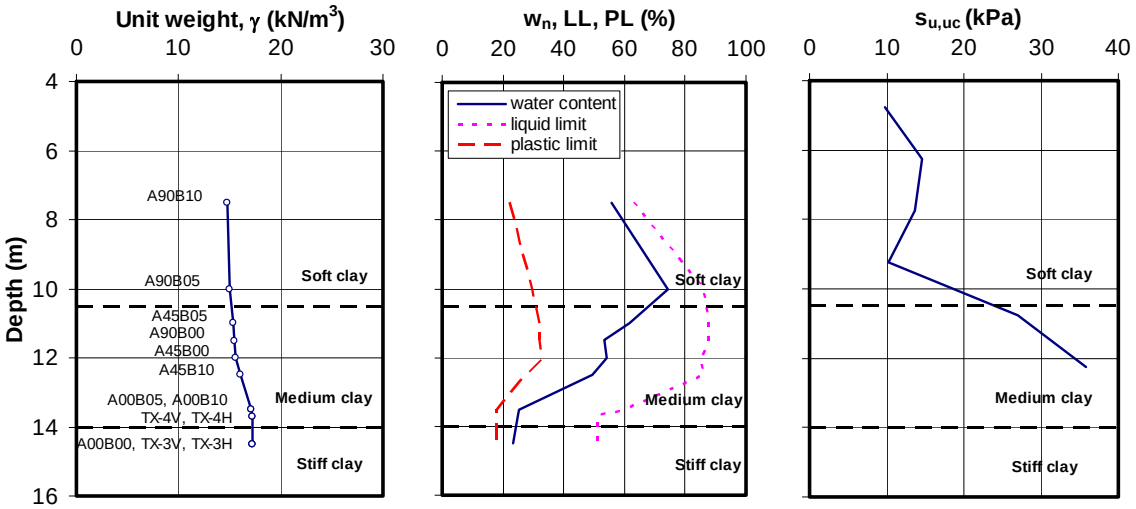

Fig. 2 Profiles of soil properties

were performed on both vertically- and horizontally-cut specimens which corresponded to the conditions of ($\alpha=0°$, $b=0$) and ($\alpha=90°$, $b=0$), respectively. The stress paths in deviatoric plane of all tests are shown in Fig. 3.

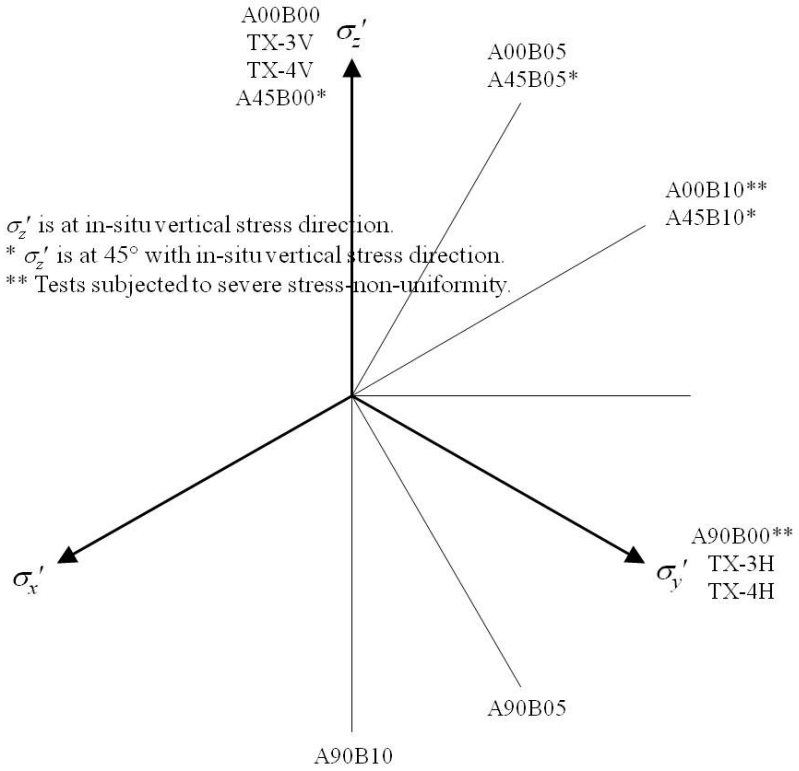

Fig. 3 Stress paths in deviatoric plane

Table 1 Torsional shear hollow cylinder test program

Test No.	Depth (m)	w_n (%)	e_o	p_o' (kPa)	α (°)	b
A00B00	14.5	20.2	0.54	105	0	0
A00B05	13.5	22.2	0.59	100	0	0.5
A00B10	13.5	25.3	0.67	100	0	1
A45B00	12.0	54.3	1.44	85	45	0
A45B05	11.0	61.8	1.64	75	45	0.5
A45B10	12.5	49.4	1.31	90	45	1
A90B00	11.5	53.4	1.42	85	90	0
A90B05	10.0	79.3	2.10	65	90	0.5
A90B10	7.5	55.6	1.47	45	90	1

*p_o' = isotropic mean stress; w_n = natural water content

Table 2 Triaxial test program

Test No.	Specimen direction	Depth (m)	w_n (%)	e_o	p_o'	α (°)	b
TX-3V	Vertical	14.5	27.7	0.73	130	0	0
TX-4V	Vertical	13.7	29.3	0.78	120	0	0
TX-3H	Horizontal	14.5	23.5	0.62	130	90	0
TX-4H	Horizontal	13.7	25.0	0.66	120	90	0

Although, TSHC apparatus can control the magnitude and direction of the major and minor principal stresses while independently varying the magnitude of the intermediate principal stress, it achieves this with the expense of stress-nonuniformity across the specimen wall. Applications of difference in external and internal pressures and/or torque cause nonuniformity, the degree of which depends on the stress state, specimen dimensions, soil stiffness, and constitutive law of the soil. Investigations into the stress-nonuniformity in TSHC specimens were reported by Hight *et al*. (1983) and Sayao and Vaid (1991) using linear elastic soil model. Wijewickreme and Vaid (1991) revealed that for a given stress state, a linear elastic assumption overestimated the stress-nonuniformity in the TSHC specimen and the nonlinear elastic assumption yielded much larger domain of general stress space that can be explored using TSHC device. It has been pointed out, however, that stress-nonuniformity across the wall of the TSHC specimen would always be expected in the vicinity of the corners ($\alpha=0°, b=1$) and ($\alpha=90°$, $b=0$) where the value of (p_o-p_i) is high and with lesser degree in the regions where M_T is high (i.e., in the vicinity of $\alpha=45°$). In the current TSHC program, there were 2 tests which were likely to suffer from stress-nonuniformity problem, i.e., A00B10 and A90B00. However, the TSHC test A90B00 can be supplemented with TX test TX-3H and TX-4H, all of which have identical stress conditions. These tests with severe stress-nonuniformity are noted and taken into account in following discussion.

3. Stress-strain and pore pressure behaviors

Fig. 4 presents the stress-strain curves from TSHC in terms of normalized deviatoric stress (q/p_o') versus deviatoric strain (ε_q), the definitions of which are shown in Eqs. (3) and (4), respectively. At any b, Bangkok Clay tends to exhibit a softer response when the major principal stress becomes more horizontal (α increases) with more pronounced effects when α increases from 0° to 45°. The value of b has relatively less effects on the stress-strain curves. The effects of α on stress-strain curves found in this study are similar to TSHC data reported by Zdravkovic and Jardine (2000) on quartzitic silt and Kumruzzaman and Yin (2010) on sandy silt. The effects of b on stress-strain curves found in this study are similar to TTX data reported by Prashant and Penumadu (2005, 2007) on reconstituted kaolin. Fig. 5 presents TX and TSHC results of comparable conditions. It can be seen that TSHC results show more anisotropic characteristics than those of TX (TSHC > TX at $\alpha=0°$, whereas TSHC < TX at $\alpha=90°$), the reasons of which may be that: (i) the A90B00 specimen has a tendency to suffer from stress-nonuniformity and to a lesser extent that (ii) A90B00 specimen is taken from softer stratum than other specimens; therefore, it tends to yield softer response. Moreover, the results from this study are comparable to the TX results (CK_oUC) of stiff Bangkok Clay specimen (at 18.5 m depth) reported by Shibuya *et*

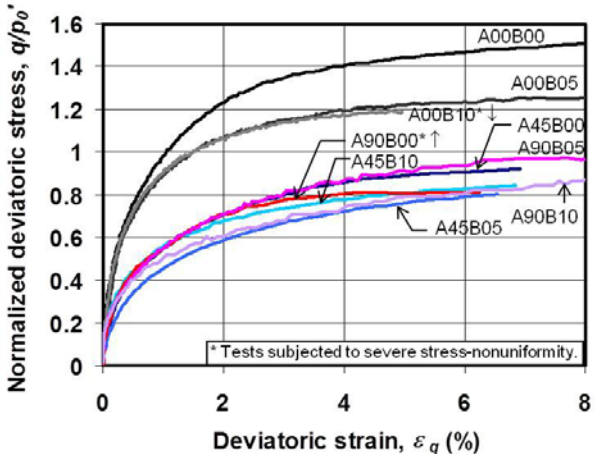

Fig. 4 Stress-strain curves at different α and b

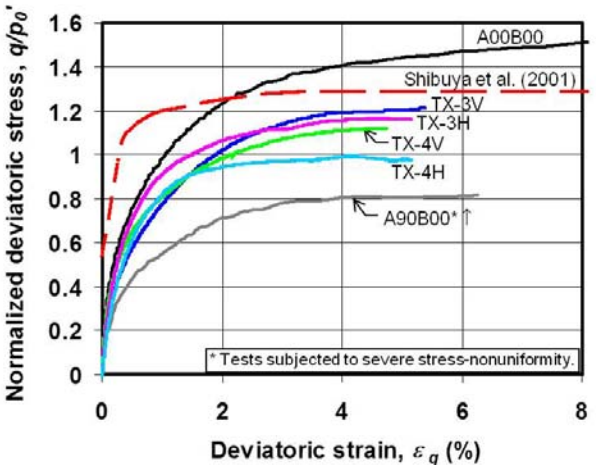

Fig. 5 Comparison of stress-strain curves

al. (2001). Some differences in the observed stiffness may be due to the difference in consolidation conditions.

$$q = \sqrt{3J_2} = \frac{1}{\sqrt{2}}\sqrt{(\sigma_1 - \sigma_2)^2 + (\sigma_2 - \sigma_3)^2 + (\sigma_1 - \sigma_3)^2} \tag{3}$$

$$\varepsilon_q = \frac{\sqrt{2}}{3}\sqrt{(\varepsilon_1 - \varepsilon_2)^2 + (\varepsilon_2 - \varepsilon_3)^2 + (\varepsilon_1 - \varepsilon_3)^2} \tag{4}$$

Fig. 6 presents the excess pore pressure data in terms of normalized excess pore pressure ($\Delta u/p_o'$) versus deviatoric strain (ε_q). It is noted that Δu of TSHC is from constant p test which excludes the effects of change in p during shearing. At any b, Bangkok Clay tends to exhibit a more contractive response when the major principal stress becomes more horizontal (α increases)

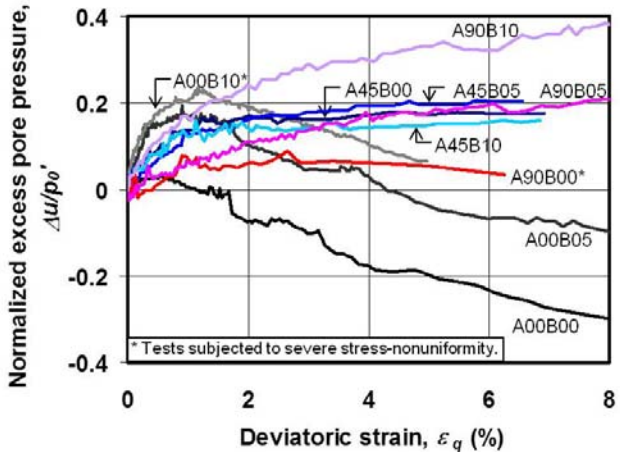

Fig. 6 Excess pore pressure curves at different α and b

with more pronounced effects when α increases from 0° to 45°. Bangkok Clay also becomes more contractive as the value of b increases but the effects of b cannot be observed for the case of α = 45°. The effects of α on excess pore pressure found in this study are similar to TSHC data reported by Zdravkovic and Jardine (2000) on quartzitic silt and Kumruzzaman and Yin (2010) on sandy silt and also similar to TTX data reported by Kuwano and Bhattarai (1989) on undisturbed Bangkok Clay and Prashant and Penumadu (2005) on reconstituted kaolin. The effects of b on excess pore pressure found in this study are similar to TSHC data reported by Kumruzzaman and Yin (2010) on sandy silt and TTX data reported by Prashant and Penumadu (2004, 2007) on reconstituted kaolin. Fig. 6 presents TX (excluding effects of change in p) and TSHC results of comparable conditions. It can be seen that TSHC results show more anisotropic characteristics than those of TX (TSHC < TX at α = 0°, whereas TSHC > TX at α = 90°), the reasons of which have been discussed earlier.

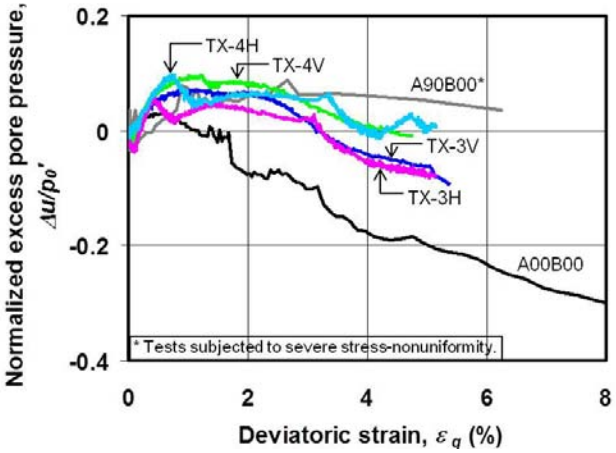

Fig. 7 Comparison of excess pore pressure curves

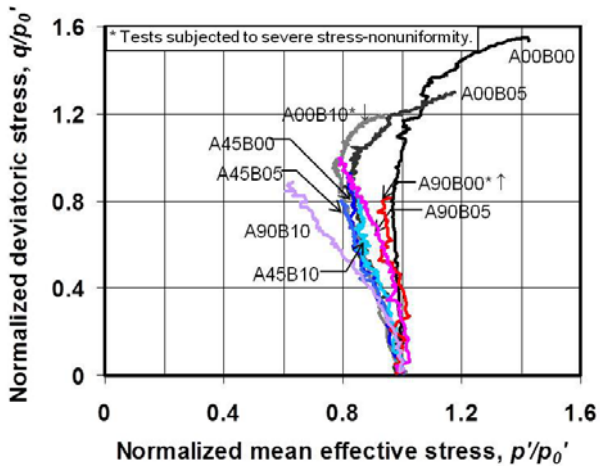

Fig. 8 Stress paths at different α and b

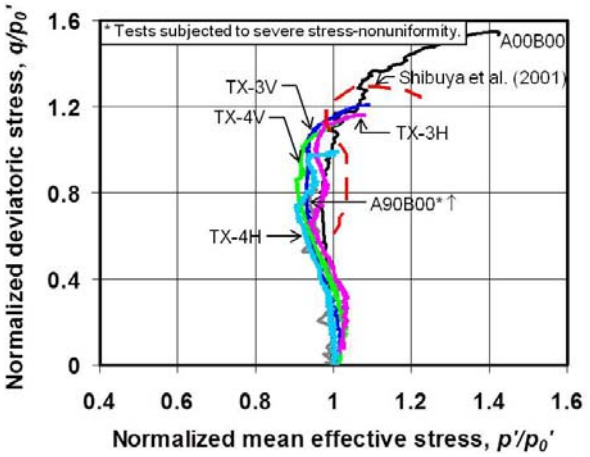

Fig. 9 Comparison of stress paths

Fig. 8 presents stress paths in terms of normalized deviatoric stress (q/p_o') versus normalized mean effective stress (p'/p_o'). The results show that α has relatively no effect on the stress path characteristics. The stress path at $\alpha = 0°$ (A00B00) shows dilative behavior after reaching maximum excess pore pressure which makes the stress path turn right with increasing deviatoric stress. However, the stress paths have tendency to move to the left as b increases due to the generation of more excess pore pressure except for the case of $\alpha = 45°$. The effects of b on stress path found in this study are similar to TSHC data reported by Kumruzzaman and Yin (2010) on sandy silt. Fig. 9 presents TX and TSHC results of comparable conditions together with TX results of Shibuya *et al.* (2001). All data show conforming trends.

4. Strength and stiffness behaviors

Fig. 10 summarized the effects of α and b on normalized undrained shear strength (s_u / p_o') (where $s_u = q_{max}/2$). Fig. 10(a) shows that Bangkok Clay has lower s_u / p_o' when the major principal stress becomes more horizontal (α increases) with less pronounced effects when α increases from 45° to 90°. The values of s_u / p_o' from TX seem to be less affected by α (more isotropic) due to the reasons discussed earlier. Fig. 10(b) shows that s_u / p_o' decreases as b increases for $\alpha = 0°$ but with less effects of b when $\alpha = 45°$ and 90°. The CK_oUC data of stiff Bangkok Clay reported by Shibuya *et al*. (2001) and CK_oUC/E data of medium Bangkok Clay reported by Seah and Lai (2003) also show relatively consistent results with this study. The effects of α on s_u / p_o' found in this study are similar to TSHC data reported by Zdravkovic and Jardine (2000) on quartzitic silt and TTX data reported by Prashant and Penumadu (2005) on reconstituted kaolin. The effects of b on s_u / p_o' found in this study are similar to TTX data reported by Kirkgard and Lade (1993) on undisturbed San Francisco Bay Mud and Prashant and Penumadu (2007) on reconstituted OC kaolin. Some

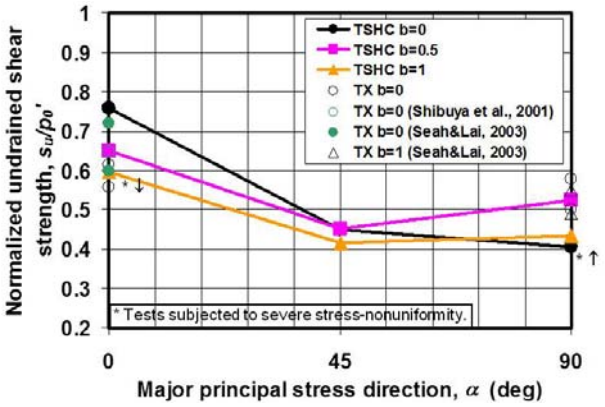

(a) Effects of α

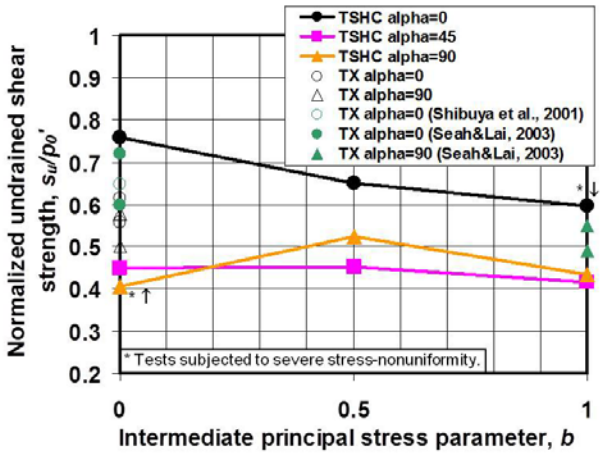

(b) Effects of b

Fig. 10 Effects of α and b on s_u/p_0'

remarks should be made here that there was non-conformity of definitions of undrained shear strength among the literatures. Some define s_u in two-dimension ($s_u = (\sigma_1 - \sigma_3)/2$), whereas some define s_u in three-dimension (s_u is a function of J_2).

Fig. 11 summarizes the effects of α and b on normalized excess pore pressure at failure ($\Delta u_f / p_o'$). The value of Δu_f is the excess pore pressure from constant p test and taken at ε_q = 6%. Fig. 11(a) shows that $\Delta u_f / p_o'$ increases as the major principal stress becomes more horizontal (α increases) with less pronounced effect when α increases from 45° to 90°. Fig. 11(b) shows that $\Delta u_f / p_o'$ increases as the value of b increases but the effects of b cannot be observed for the case of α = 45°. The values of $\Delta u_f / p_o'$ from TX (excluding effect of change in p) are also relatively consistent with TSHC results but they are less affected by α (more isotropic) due to the reasons discussed earlier. The CK_oUC/E data of Seah and Lai (2003) also show similar results.

Fig. 12 shows the effects of α on the variation of friction angle (ϕ_f') and stress ratio at failure (M_f). The friction angle (ϕ') and stress ratio (M) are calculated as defined in Eqs. (5) and (6),

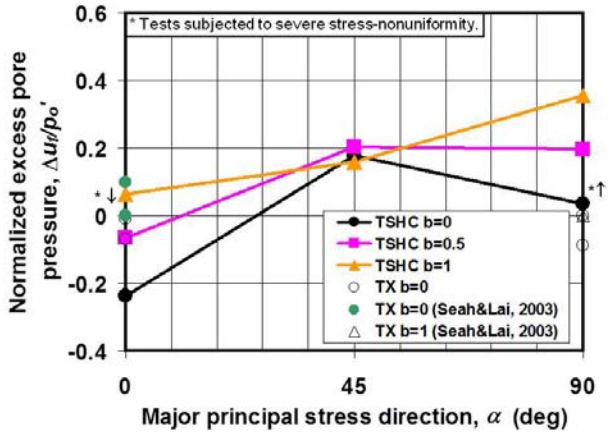

(a) Effects of α

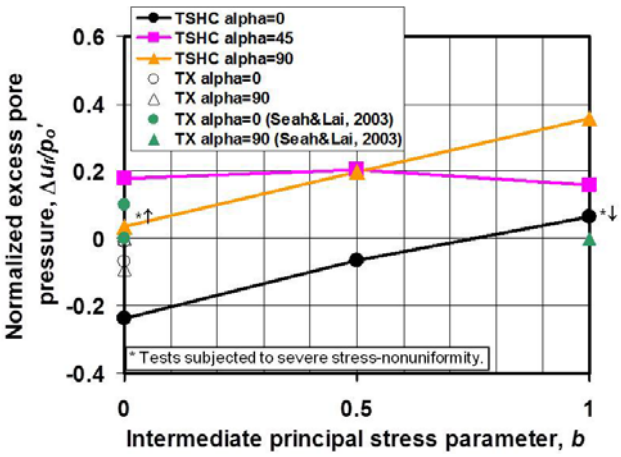

(b) Effects of b

Fig. 11 Effects of α and b on $\Delta u_f / p_0'$

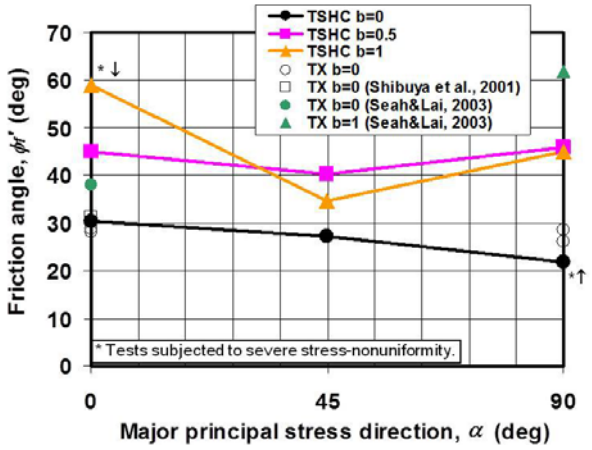

(a) Friction angle

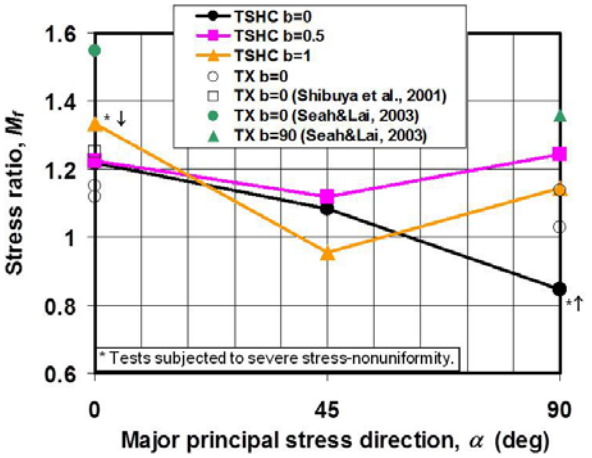

(b) Stress ratio

Fig. 12 Effects of α on ϕ_f' and M_f

respectively. The failure condition in this analysis is defined as the points of peak deviatoric stress. The results show that both ϕ_f' and M_f have non-monotonic relationships with α and they have the lowest values at approximately $\alpha = 45°$. Fig. 13 shows the effects of b on the variation of ϕ_f' and M_f. The results show that ϕ_f' increases with b especially when b changes from 0 to 0.5, whereas M_f is relatively constant with b. The results of TX from this study, Shibuya *et al*. (2001), and Seah and Lai (2003) are consistent with TSHC data but with more isotropic characteristics. The effects of α on ϕ_f' found in this study are similar to TSHC data of undisturbed London Clay which show a minimum of ϕ_f' at $\alpha \approx 45°$-$48°$ (Nishimura *et al*. 2007) and also similar to PS data on reconstituted kaolin which show a minimum of ϕ_f' at $\alpha \approx 60°$ (Kurukulasuriya *et al*. 1999). However, some studies reported a monotonically decrease of ϕ_f' against an increase in α (e.g., Zdravkovic and Jardine 2000 and Kumruzzaman and Yin 2010). The effects of b on ϕ_f' found in this study are similar to the data reported by other studies (e.g., Kuwano and Bhattarai 1989, Kirkgard and Lade

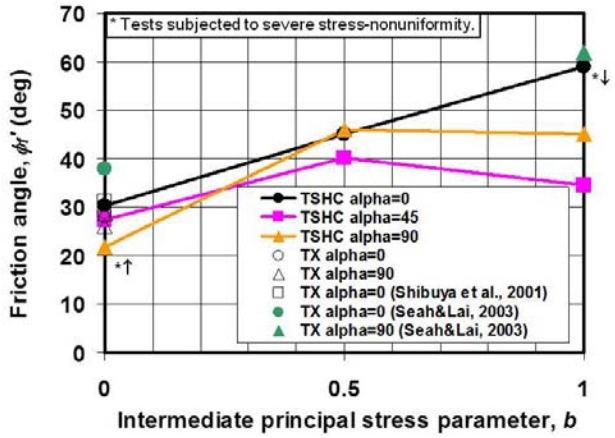

(a) Friction angle

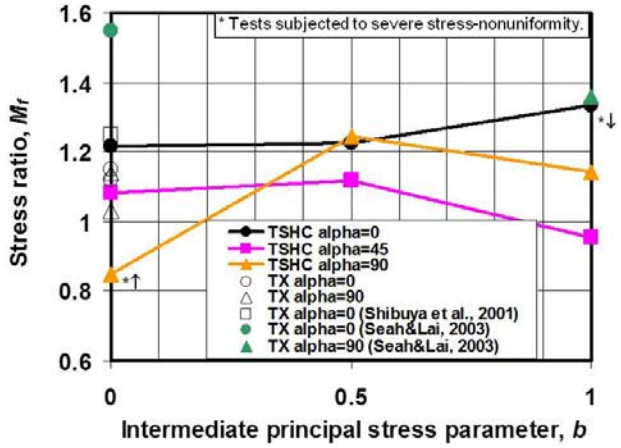

(b) Stress ratio

Fig. 13 Effects of b on ϕ_f' and M_f

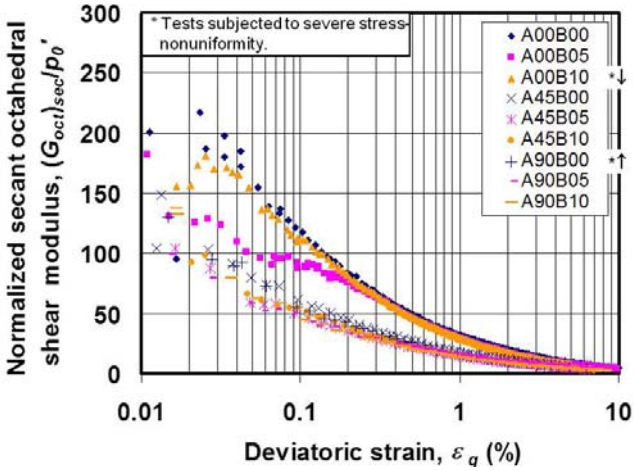

Fig. 14 Normalized secant shear stiffness degradation curves at different α and b

1993, Zdravkovic and Jardine 2000, Prashant and Penumadu 2007, and Kumruzzaman and Yin 2010).

$$\phi' = \sin^{-1}\left(\frac{\sigma_1' - \sigma_3'}{\sigma_1' + \sigma_3'}\right) \tag{5}$$

$$M = \frac{6\sin\phi'\sqrt{1-b+b^2}}{3+(2b-1)\sin\phi'} \tag{6}$$

Fig. 14 presents shear modulus degradation curves in terms of normalized secant octahedral shear modulus ($(G_{oct})_{sec}/p_o'$) versus deviatoric strain (ε_q). The octahedral shear modulus (G_{oct}) is calculated as defined in Eq. (7). The stiffness data from TSHC can be measured to the strain of as small as 0.01%. The results show that G_{oct} gradually decreases as ε_q increases due to the non-linear nature of soil. Moreover, Bangkok Clay becomes less stiff as the major principal stress becomes more horizontal (α increases) but this cannot be clearly observed for the case of $b = 0.5$. The b value has relatively no effects on stiffness.

$$G_{oct} = \frac{\Delta q}{3\Delta\varepsilon_q} \tag{7}$$

Fig. 15 summarizes the variation of ($(G_{oct})_{sec}/p_o'$) at ε_q = 0.01% with α and b. The results show that the normalized shear modulus decreases when the major principal stress becomes more horizontal (α increases) but the effects are not so obvious when α increases from 45° to 90°. The normalized shear modulus seems to decrease with an increase in b but the effects are relatively small. The relatively small effects of b on the normalized shear modulus found in this study are quite different from other studies which report that, as b increases, the stiffness either increases (e.g., Kuwano and Bhatarai 1989, Kirkgard and Lade 1993, and Prashant and Penumadu 2004) or decreases (e.g., Zdravkovic and Jardine 2000).

The undrained stiffness anisotropy is presented in Fig. 16 which shows undrained Young's modulus degradation curves in terms of normalized secant undrained Young's modulus ($E_{u,sec}/p_o'$) versus axial strain (ε_a). The $E_{u,sec}$ is calculated as $\Delta\sigma_1/\Delta\varepsilon_1$ and ε_a is equal to ε_1. This definitions are considered justified for $\alpha = 0°$ and 90° since σ_1 and ε_1 have similar directions for these conditions. The results of TSHC and TX of comparable conditions ($\alpha = 0°$ and 90° with $b = 0$) are presented. The TX results can investigate the data for strains as small as 0.001% due to the virtue of local measurement systems, whereas the TSHC results can show the data for strain as small as only 0.01%. The TSHC and TX results show similar anisotropic stiffness characteristics where Bangkok Clay is stiffer in vertical direction under undrained condition. The ratio of $E_{u,0}/E_{u,90}$ at ε_a = 0.01% from TSHC data is approximately 1.5, whereas the ratio of $E_{u,0}/E_{u,90}$ at ε_a = 0.001% and 0.01% from TX data is approximately 1.7. These ratios can be compared with those of other undisturbed clays as shown in Table 3. It can be seen that the undrained Young's modulus anisotropy of Bangkok Clay, which is lightly-overconsolidated clay, is opposite to those of London Clay and Gault Clay, which are heavily-overconsolidated clays. Under undrained condition, Bangkok Clay is stiffer in vertical direction, whereas London Clay and Gault Clay are stiffer in horizontal direction. However, it is interesting to note that the reported value of San Francisco Bay Mud, which is also lightly-overconsolidated clay, is similar to those of London Clay and Gault Clay rather than that of Bangkok Clay.

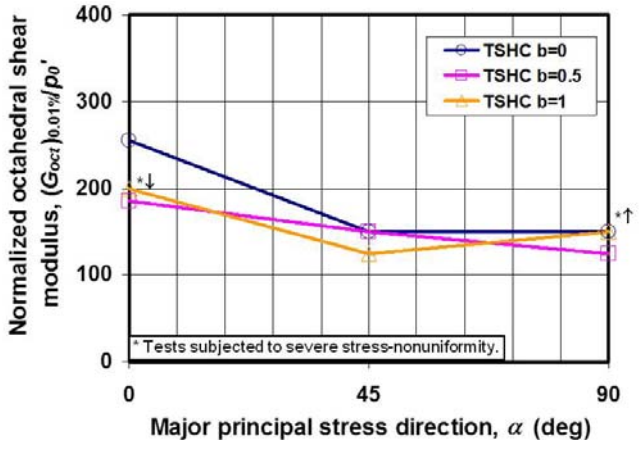

(a) Effects of α

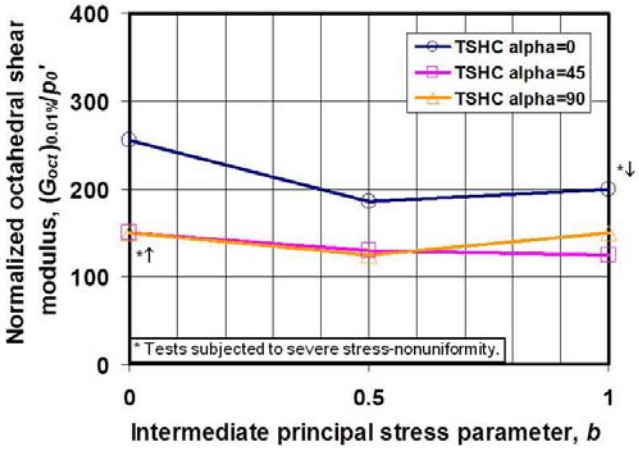

(b) Effects of b

Fig. 15 Effects of α and b on $(G_{oct})_{0.01\%}/p_o'$

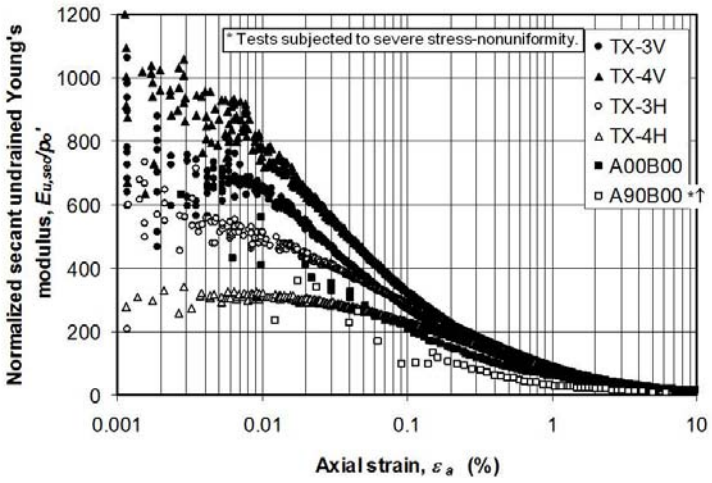

Fig. 16 Effects of α on $E_{u,sec}/p_o'$

Table 3 Ratios of $E_{u,0}/E_{u,90}$

Soil	$E_{u,0}/E_{u,90}$	Strain range	References
Bangkok Clay	1.5 – 1.7	Intermediate	This study
	1.6	Small	Ratananikom *et al*. (2013)
	1.7	Small	This study
San Francisco Bay Mud	0.7	Intermediate	Kirkgard and Lade (1991)
London Clay	0.8	Intermediate	Atkinson (1975)
	0.6	Small	Yimsiri and Soga (2011)
Gault Clay	0.6	Small	Lings (2001)
	0.6	Small	Yimsiri and Soga (2011)

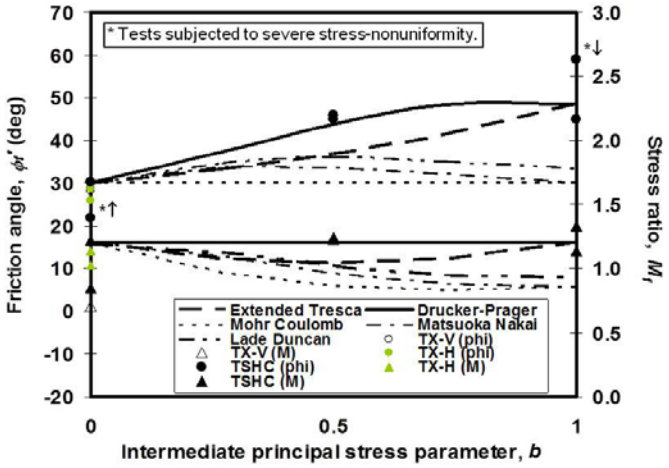

(a) α = 0° and 90°

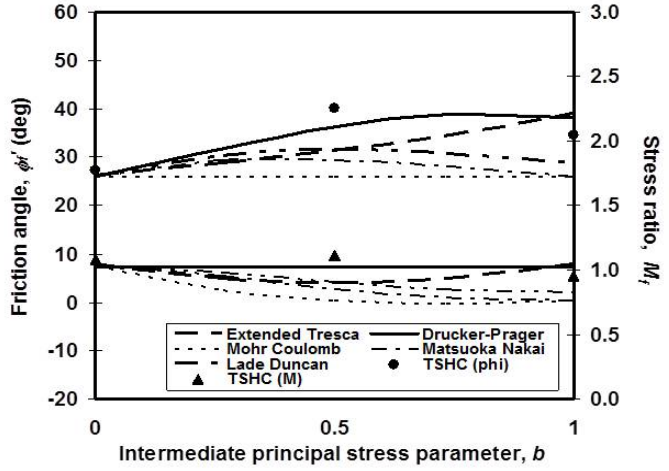

(b) α = 45°

Fig. 17 Variation of ϕ_f' and M_f versus b parameter

5. Failure criterion

Fig. 17 shows the variations of ϕ_f' and M_f with b parameter of 2 cases, i.e., (a) $\alpha = 0°$ and 90°; and (b) $\alpha = 45°$. The prediction of ϕ_f' and M_f by five commonly quoted failure criteria are also superimposed in these figures by fitting the model with the results of triaxial compression conditions. The details of the failure criteria and the parameters used are summarized in Table 4.

Table 4 Failure criteria (after Potts and Zdravkovic 1999)

Failure criteria		Parameters
	Mohr-Coulomb model	
Failure criterion:	$f = \sqrt{3J_2} - M(\theta)(p' + c'\cot\phi') = 0$	$c' = 0$
where	$M(\theta) = \dfrac{3\sin\phi'}{\sqrt{3}\cos\theta + \sin\theta\sin\phi'}$	ϕ' = 32° (for $\alpha = 0°$ and 90°) = 27° (for $\alpha = 45°$)
	Extended Tresca model	
Failure criterion:	$f = \sqrt{J_2}\cos\theta - k = 0$	k = 65 kPa (for $\alpha = 0°$ and 90°) = 54 kPa (for $\alpha = 45°$)
where	$M(\theta) = \dfrac{\sqrt{3}k}{p'\cos\theta}$	
	Drucker-Prager model	
Failure criterion:	$f = \sqrt{3J_2} - M(\phi')(p' + c'\cot\phi') = 0$	$c' = 0$
where	$M(\phi') = \dfrac{6\sin\phi'}{3 - \sin\phi'}$	ϕ' = 32° (for $\alpha = 0°$ and 90°) = 27° (for $\alpha = 45°$)
	Lade-Duncan model	
Failure criterion:	$f = \sqrt{3J_2} - M(\theta)(p' + c'\cot\phi') = 0$	$c' = 0$ ϕ' = 32° (for $\alpha = 0°$ and 90°) = 27° (for $\alpha = 45°$)
where $M(\theta)$ are roots of:	$2M(\theta)^3\sin 3\theta + 9M(\theta)^2 - 10.67 = 0$	$\eta = 27.40$, $m = 0.40$
	Matsuoka-Nakai model	
Failure criterion:	$f = \sqrt{3J_2} - M(\theta)(p' + c'\cot\phi') = 0$	$c' = 0$ ϕ' = 32° (for $\alpha = 0°$ and 90°) = 27° (for $\alpha = 45°$)
where $M(\theta)$ are roots of:	$24.25M(\theta)^3\sin 3\theta + 82.11M(\theta)^2 - 84.32 = 0$	

*Note: θ = Lode angle

$$\phi' = \sin^{-1}\left[\frac{3M}{6\sqrt{1 - b + b^2} - (2b - 1)M}\right]$$

The results show that the variations of ϕ_f' and M_f can be best approximated by the Drucker-Prager failure criterion. Furthermore, the failure conditions of Bangkok Clay are also presented in deviatoric plane for a constant mean effective stress of $p' = 100$ kPa as shown in Fig. 18 for 2 cases, i.e., (a) $\alpha = 0°$ and 90°; and (b) $\alpha = 45°$ (see also Fig. 1). Fig. 18(a) ($\alpha = 0°$ and 90°) shows the failure points symmetrically about the vertical axis (σ_z') due to the hypothesis of cross-anisotropy of the specimen obtained from the field (Ratananikom *et al*. 2013). The five commonly quoted failure envelopes, the details of which are shown in Table 4, are compared with the experimental data. Again, it can be seen that the Drucker-Prager failure criterion shows best fit to the experimental data. It is noted that the results of A90B00 (on σ_x'- and σ_y'-axis) are smaller and do not fit the proposed failure criterion well, which may be due to stress-nonuniformity. Fig. 18(b) ($\alpha = 45°$) has the experimental data for only 1/6 of the full failure envelope; however, failure points are plotted in six-fold symmetry about the origin due to the hypothesis of isotropy which is postulated from the case of $\alpha = 0°$ and 90°. It can be seen that the Drucker-Prager failure criterion still fits the results well. The Drucker-Prager failure criterion found for undisturbed Bangkok Clay from this study is consistent with the TTX data of similar soil reported earlier by Kuwano and Bhattarai (1989). However, other studies on undisturbed clays report that their failure envelopes are rather similar to Lade-Duncan type and also show anisotropic characteristics (e.g., Kirkgard and Lade 1993, Callisto and Callabresi 1998, and Callisto and Rampello 2002).

Fig. 18 also presented the plastic strain increment vectors on the principal strain axes which are superimposed on the principal stress axes. The plastic strain increments are taken at $\varepsilon_q \approx 5\%$ to avoid effects of strain non-uniformity and it is assumed that the strains at this stage are fully plastic. The results show that the strain increment vectors appear to be normal to the Drucker-

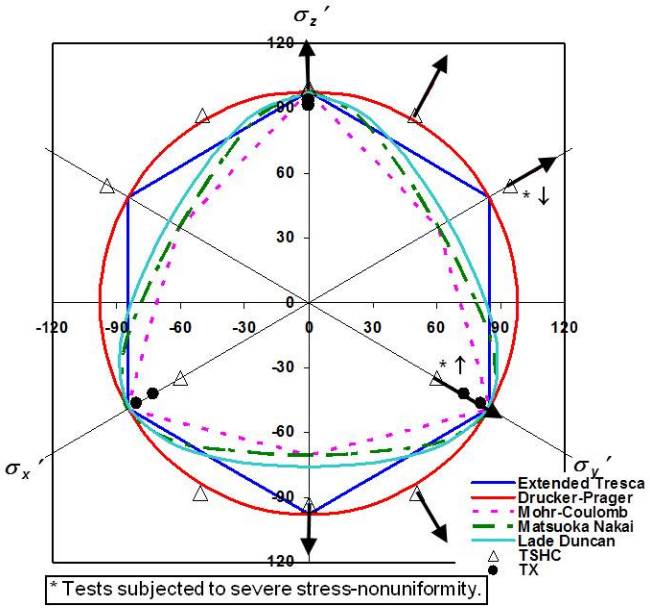

(a) $\alpha = 0°$ and 90°

Fig. 18 Failure surface on deviatoric plane of Bangkok Clay

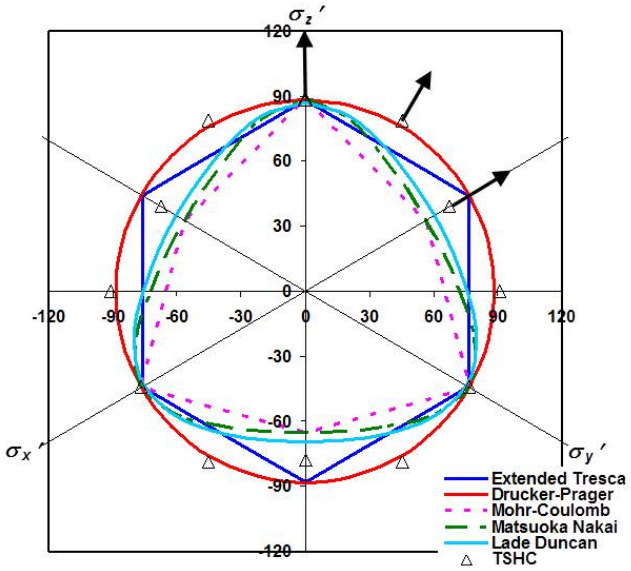

(b) $\alpha = 45°$

Fig. 18 Continued

Prager failure envelope. This indicates that the failure envelope and the plastic potential are identical corresponding to an associated flow rule. This finding is also consistent with the data of undisturbed Bangkok Clay reported earlier by Kuwano and Bhattarai (1989). Other studies on undisturbed clays report that their plastic flow rules are both associative (e.g., Callisto and Calabresi 1998) and non-associative (e.g., Kirkgard and Lade 1993, and Callisto and Rampello 2002).

6. Relationship between individual strain components

Fig. 19 shows relationships between strain components of tests with $b = 0.5$. These tests are performed in order to investigate plane-strain condition where ε_2 is supposed to be negligible. It can be seen that the case of A45B05 shows very small development of ε_2; however, the cases of A00B05 and A90B05 show some development of ε_2 toward the final stage of the test. The results may imply that the plane-strain condition corresponds to b of slightly less than 0.5 for $\alpha = 45°$ and corresponds to lower b values for $\alpha = 0°$ and 90°. This finding is consistent with the data of undisturbed Bangkok Clay by Kuwano and Bhatarai (1989) who reported that $b = 0.27$-0.5 for plane-strain condition. Other studies also reported $b = 0.2$-0.66 for plane-strain condition (e.g., Kirkgard and Lade 1993, Zdravkovic and Jardine 1997, and Prashant and Penumadu 2004).

Fig. 19(b) ($\alpha = 45°$, $b = 0.5$) corresponds to conditions where σ_z, σ_r, σ_θ are constant with $\tau_{\theta z}$ continually increasing during the test. It is evident that only the shear strain component $\gamma_{\theta z}$ dominates during early stage of the test and the normal strain components ε_z, ε_θ, and ε_r remain negligible which means that the development of shear stress during the test has no effect on any

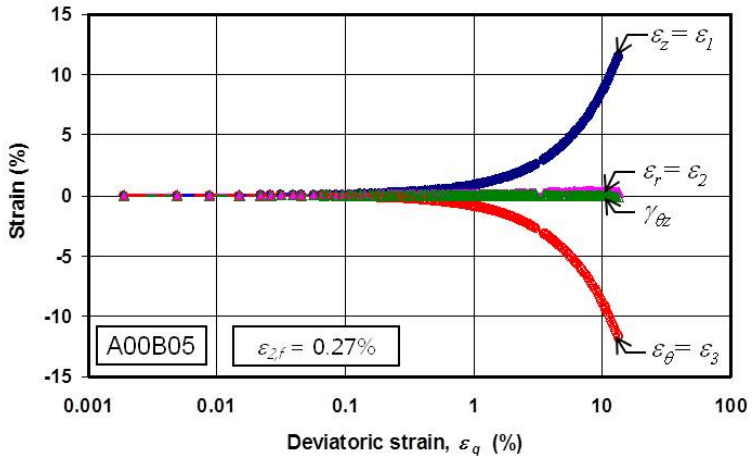

(a) A00B05

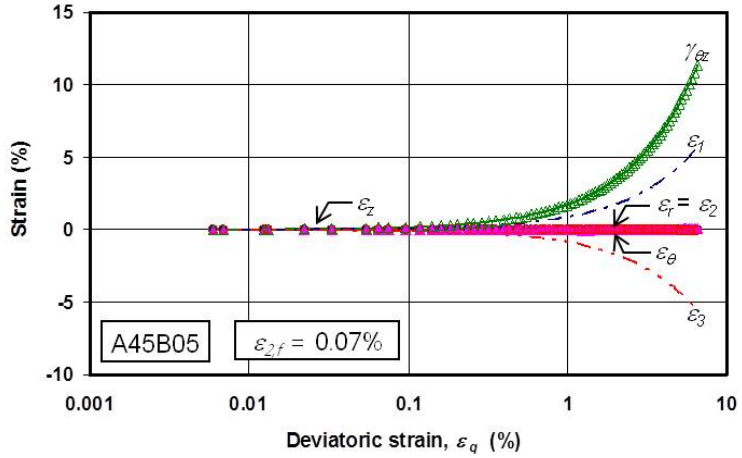

(b) A45B05

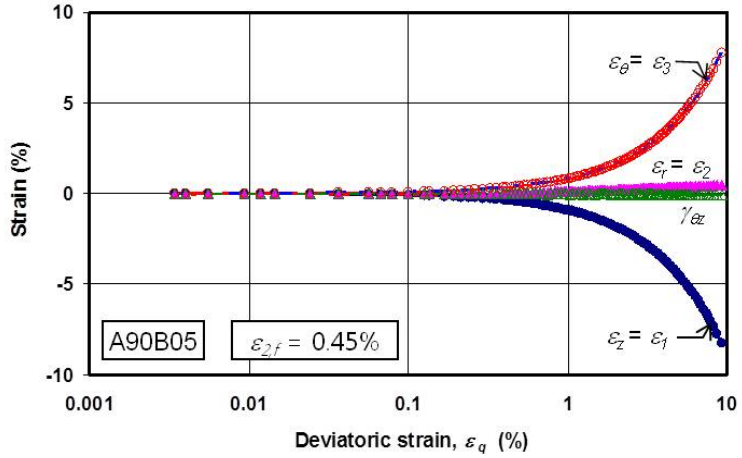

(c) A90B05

Fig. 19 Relationships between individual strains

normal strains. Considering the conventional cross-anisotropic elastic equation of total stress for TSHC condition as shown in Eq. (8) with reciprocal rule, this implies that the six cross-coupling terms in the compliance matrix can be taken as zero. Moreover, according to principle of effective stress, the compliance matrix in terms of effective stress also has identical form.

$$\begin{pmatrix} \Delta\varepsilon_z \\ \Delta\varepsilon_r \\ \Delta\varepsilon_\theta \\ \Delta\gamma_{z\theta} \end{pmatrix} = \begin{pmatrix} \frac{1}{E_z} & \frac{\nu_{rz}}{E_r} & \frac{\nu_{\theta z}}{E_\theta} & 0 \\ \frac{\nu_{zr}}{E_z} & \frac{1}{E_r} & \frac{\nu_{\theta r}}{E_\theta} & 0 \\ \frac{\nu_{z\theta}}{E_z} & \frac{\nu_{r\theta}}{E_r} & \frac{1}{E_\theta} & 0 \\ 0 & 0 & 0 & \frac{1}{G_{z\theta}} \end{pmatrix} \begin{pmatrix} \Delta\sigma_z \\ \Delta\sigma_r \\ \Delta\sigma_\theta \\ \Delta\tau_{z\theta} \end{pmatrix} \tag{8}$$

Fig. 20 presents the evolution of principal stress and strain directions together with principal stress increment and principal strain increment directions during undrained shearing. The definitions of directional parameters are given in Eqs. (9) to (12). In all tests, the principal stress direction is constant throughout the tests; therefore, the principal stress direction is identical to the principal stress increment direction ($\alpha = \alpha_{\sigma'}$). The results show that all tests with the principal stress directions coinciding with the principal axes of the material ($\alpha = 0°$ and 90°) show coincidence of the principal stress increment and principal strain inclement directions. The example of these cases is presented in Fig. 20(a) for test A00B00. The tests which involve rotation of the principal stress

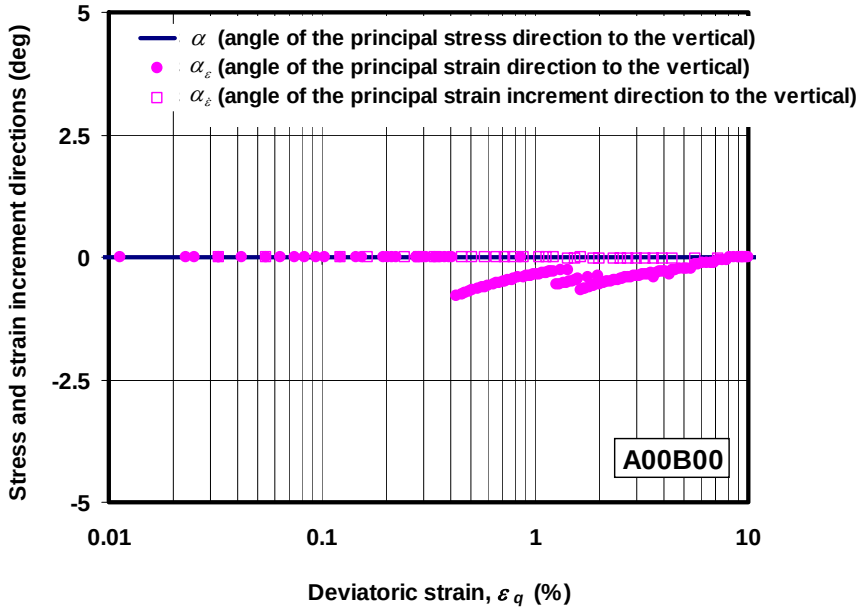

(a) A00B00

Fig. 20 Evolutions of principal stress and strain increment directions

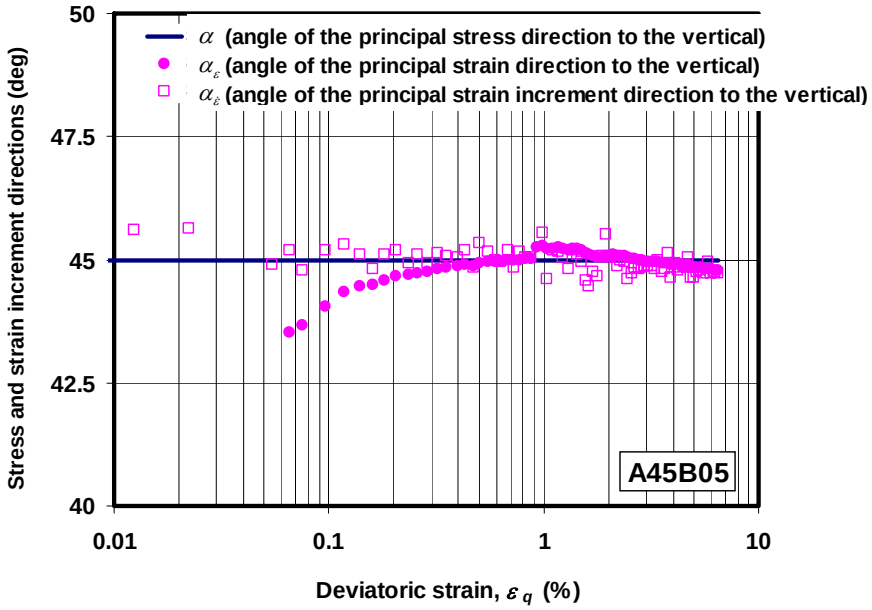

(b) A45B05

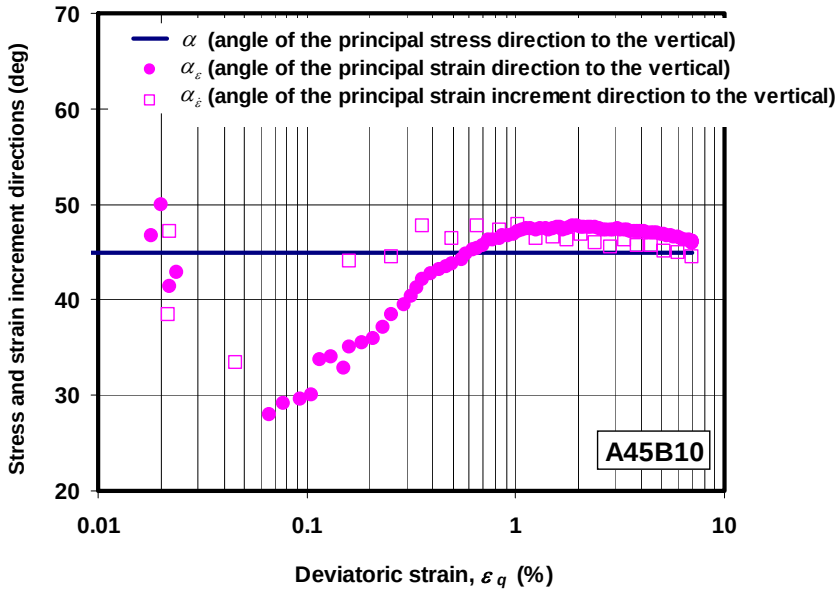

(c) A45B10

Fig. 20 Continued

direction away from the principal axes of the material (cases with $\alpha = 45°$) show some deviation between the principal stress increment and principal strain increment directions. For tests A45B00 and A45B05, the principal stress increment and principal strain increment directions show small

deviation of up to $\pm 2°$ at $\varepsilon_q = 0.06\%$ as shown in Fig. 20(b). However, test A45B10 shows a difference of up to $\pm 17°$ during the beginning of shearing stage ($\varepsilon_q = 0.06\%$) before gradually converging to remain within $\pm 1°$ after ε_q exceeds ~3% as shown in Fig. 20(c). The difference of the observed principal stress increment and principal strain increment directions during the beginning of shearing (small- to intermediate-strain range) is due to the cross-anisotropic elastic characteristics of the material. Subsequently, during undrained shearing, both directions are gradually converging due possibly to: (i) the adjustment of principal axes of the material to coincide with the principal stress increment direction and (ii) the evolution of plastic behavior. This observed behavior during undrained shearing is similar to the results during inclined consolidation of quartzitic silt reported by Zdravkovic and Jardine (2001).

Principal stress direction
$$\alpha = \frac{1}{2}\tan^{-1}\left(\frac{2\tau_{z\theta}}{\sigma_z - \sigma_\theta}\right) \tag{9}$$

Principal stress increment direction
$$\alpha_{\dot{\sigma}} = \frac{1}{2}\tan^{-1}\left(\frac{2\Delta\tau_{z\theta}}{\Delta\sigma_z - \Delta\sigma_\theta}\right) \tag{10}$$

Principal strain direction
$$\alpha_{\varepsilon} = \frac{1}{2}\tan^{-1}\left(\frac{2\varepsilon_{z\theta}}{\varepsilon_z - \varepsilon_\theta}\right) \tag{11}$$

Principal strain increment direction
$$\alpha_{\dot{\varepsilon}} = \frac{1}{2}\tan^{-1}\left(\frac{2\Delta\varepsilon_{z\theta}}{\Delta\varepsilon_z - \Delta\varepsilon_\theta}\right) \tag{12}$$

7. Conclusions

This study presents the experimental study of undrained strength-deformation characteristics of Bangkok Clay under general stress state by TSHC and advanced TX apparatus. Several behaviors are investigated and discussed including: (i) stress-strain and pore pressure behaviors, (ii) stiffness characteristics, and (iii) strength characteristics. The results of all tests are summarized in Table 5. The study shows evident influences of the direction of major principal stress and the magnitude of intermediate principal stress on the observed soil behaviors which can be summarized in Table 6. Most of the experimental results from Bangkok Clay are more or less similar to previous findings reported for undisturbed and reconstituted clays. However, the result on stiffness is quite unique from other studies where it is found that b has small effects on shear stiffness. This characteristic may require further investigation.

The anisotropy of undrained Young's modulus ($E_{u,0} / E_{u,90}$) of Bangkok Clay is found to be approximately 1.5-1.7 at small- to intermediate-strain levels. It is found that the undrained Young's modulus anisotropy of Bangkok Clay is opposite to the reported values of other heavily-overconsolidated clays. However, an inconsistency is still found with the data of San Francisco Bay Mud, which is also of similar stress history to Bangkok Clay. Therefore, the effects of stress history on undrained stiffness anisotropy should require further investigation. The anisotropic elasticity is also presented in terms of the non-coincidence of principal stress

Table 5 Summary of experimental results

Test	p_o' (kPa)	s_u (kPa)	Δu_f (kPa)	ϕ_f' (°)	M_f	$(G_{oct})_{0.01\%}$ (MPa)
A00B00	105	79.6	-37	30.4	1.22	26.8
A00B05	100	65	-12.5	45	1.22	18.5
A00B10*	100	59.5 ↓	2 ↓	59 ↓	1.33 ↓	20.0 ↓
A45B00	85	38.2	15	27.3	1.08	12.8
A45B05	75	34	15.2	40.2	1.12	11.3
A45B10	90	37.5	14.4	34.6	0.95	11.3
A90B00*	85	34.6 ↑	3.5 ↑	21.8 ↑	0.85 ↑	12.8 ↑
A90B05	65	34	12.8	45.9	1.24	18.1
A90B10	45	19.5	16.8	45	1.14	6.8
TX-3V	130	80	-9.1	28.8	1.15	–
TX-4V	120	67	-1.2	28.2	1.12	–
TX-3H	130	75	-11.7	28.6	1.14	–
TX-4H	120	60	0	26.1	1.03	–

* Tests subjected to severe stress-nonuniformity

Table 6 Summary of effects of α and b

Parameters	Effects as α increases	Effects as b increases
s_u/p_o'	Decreases, especially when α increases from 0° to 45°	Somewhat decreases or constant
$\Delta u_f/p_o'$	Increases, especially when α increases from 0° to 45°	Increases, except when $\alpha = 45°$
ϕ_f'	Minimum at $\alpha = 45°$	Increases, especially when b increases from 0 to 0.5
M_f	Minimum at $\alpha = 45°$	Constant
$G_{oct,0.01\%}/p_o'$	Decreases	Small effects

increment and principal strain increment directions at small strain for tests with α = 45°. Furthermore, the results of test A45B05 ($\alpha = 45°$, $b = 0.5$) imply that the six cross-coupling terms in the elastic compliance matrix of effective stress and total stress (i.e., Eq. (8)) can be taken as zero. Therefore, the elastic behavior of Bangkok Clay can be modeled by a conventional cross-anisotropic elastic compliance matrix.

Both failure surface and plastic potential in deviatoric plane of Bangkok Clay are found to be isotropic and of circular shape which also implies associated flow rule. These results of Bangkok Clay are quite unique comparing with those of other clays. The failure envelopes of most undisturbed clays are reported to be of Lade-Duncan type with anisotropic characteristic. Moreover, the plastic flow rule in deviatoric plane of other clays is mostly non-associative. As a result, if Bangkok Clay is modeled by fitting non-circular failure surface in deviatoric plane (e.g., Mohr-Coulomb) to triaxial compression data, as commonly done in normal finite element work,

the strength analysis results of plane-strain condition should be underestimated (Grammatikopoulou *et al*. 2007). This study also reports that the plane-strain condition for Bangkok Clay is found to be at b less than 0.5 and also depends on α.

It is also found that the shapes of the failure surface in deviatoric plane still retain their circular shape with their sizes changing with the change of direction of major principal stress. This is due to the dependency of the friction angle (ϕ_f') on α. The results show that the failure surface in deviatoric plane shrinks as α increases from 0° to 45°, when it reaches its minimum, and expands as α further increases from 45° to 90°. As a result, if Bangkok Clay is modeled by fitting constant-size circular failure surface in deviatoric plane (e.g., Drucker-Prager) to triaxial compression data, as always assumed in normal analysis, the strength analysis results should be overestimated.

It is noted, however, that the results from this research provide a preliminary discussion on the behavior of Bangkok Clay under general stress condition because only a limited set of b-values (= 0, 0.5, 1) and α-values (= 0, 45, 90°) were used in the tests. There may be questions about the accuracy of the derived curved shapes of both failure surface and plastic potential in deviatoric plane. Nevertheless, this research is the first instance for Bangkok Clay where such combined loading response has been systematically investigated with explicit accounting for the variation of stress rotations and magnitudes of intermediate principal stress on an individual basis. A more comprehensive TSHC investigation supplemented with other test results, i.e., triaxial and true triaxial tests, is underway.

Acknowledgements

The CHE&AUN/SEED-Net provides the financial support during the second author's graduate study at Chulalongkorn University. This research is also supported by Thailand Research Fund (MRG 4880055).

References

Atkinson, J.H. (1975), "Anisotropic elastic deformations in laboratory tests on undisturbed London Clay", *Geotech*., **25**(2), 357-374.

Callisto, L. and Calabresi, G. (1998), "Mechanical behavior of a natural soft clay", *Geotech*., **48**(4), 495-513.

Callisto, L. and Rampello, S. (2002), "Shear strength and small-strain stiffness of a natural clay under general stress conditions", *Geotech*., **52**(8), 547-560.

Cuccovillo, T. and Coop, M.P. (1997), "The measurement of local axial strains in triaxial test using LVDTs", *Geotech*., **47**(1), 167-171.

Fukuda, F., Mitachi, T. and Shibuya, S. (1997), "Induced anisotropy appeared in the deformation and strength of remolded clay", *Soil*. *Found*., **37**(4), 139-148.

Gasparre, A., Nishimura, S., Minh, N.A., Coop, M.R. and Jardine, R.J. (2007), "The stiffness of natural London Clay", *Geotech*., **57**(1), 33-47.

Gramatikopoulou, A., Zdravkovic, L. and Potts, D.M. (2007), "The effect of the yield and plastic potential deviatoric surfaces on the failure height of an embankment", *Geotech*., **57**(10), 795-806.

Hight, D.W., Gens, A. and Symes, M.J. (1983), "The development of a new hollow cylinder apparatus for investigating the effects of principal stress rotation in soils", *Geotech*., **33**(4), 355-383.

Hird, C.C. and Yung, P.C.Y. (1989), "The Use of Proximity Transducers for Local Strain Measurements in Triaxial Tests", *Geotech*. *Test*. *J*. *ASTM*, **12**(4), 292-296.

Kirkgard, M.M. and Lade, P.V. (1991), "Anisotropy of Normally Consolidated San Francisco Bay Mud",

Geotech. Test. J. ASTM, **14**(3), 231-246.
Kirkgard, M.M. and Lade, P.V. (1993), "Anisotropic three-dimensional behavior of a normally consolidated clay", *Can. Geotech. J.*, **30**(5), 848-858.
Kumruzzaman, Md. and Yin, J.H. (2010), "Influence of principal stress direction and intermediate principal stress on the stress-strain-strength behaviour of completely decomposed granite", *Can. Geotech. J.*, **47**(2), 164-179.
Kurukulasuriya, L.C., Oda, M. and Kazama, H. (1999), "Anisotropy of undrained shear strength of an over-consolidated soil by triaxial and plane strain tests", *Soil. Found.*, **39**(1), 21-29.
Kuwano, J. and Bhattarai, B.N. (1989), "Deformation characteristics of Bangkok Clay under three dimensional stress conditions", *Geotech. Eng. SEAGS*, **20**(2), 111-137.
Lings, M.L. (2001), "Drained and undrained anisotropic elastic stiffness parameters", *Geotech.*, **51**(6), 555-565.
Nishimura, S., Minh, N.A. and Jardine, R.J. (2007), "Shear strength anisotropy of natural London Clay", *Geotech.*, **57**(1), 49-62.
Phien-Wej, N., Giao, P.H. and Nutalaya, P. (2006), "Land subsidence in Bangkok, Thailand", *Eng. Geol.*, **82**(4), 187-201.
Potts, D.M. and Zdravkovic, L. (1999), *Finite Element Analysis in Geotechnical Engineering: Theory*, Thomas Telford.
Prashant, A. and Penumadu, S. (2004), "Effect of intermediate principal stress on overconsolidated kaolin clay", *J. Geotech. Geoenviron. Eng. ASCE*, **130**(3), 284-292.
Prashant, A. and Penumadu, D. (2005), "A laboratory study of normally consolidated kaolin clay", *Can. Geotech. J.*, **42**(1), 27-37.
Prashant, A. and Penumadu, S. (2007), "Effect of microfabric on mechanical behavior of kaolin clay using cubical true triaxial testing", *J. Geotech. Geoenviron. Eng. ASCE*, **133**(4), 433-444.
Prust, R.E., Davies, J. and Hu, S. (2005), "Pressuremeter Investigation for Mass Rapid Transit in Bangkok, Thailand", *Transportation Research Record: J. Transport. Res. Board*, No. 1928, 207-217.
Ratananikom, W., Likitlersuang, S. and Yimsiri, S. (2013), "An investigation of anisotropic elastic parameters of Bangkok Clay from vertical and horizontal cut specimens", *Geomech. Geoeng.: Int.*, **8**(1), 15-27.
Sayao, A. and Vaid, Y.P. (1991), "A critical assessment of stress nonuniformities in hollow cylinder test specimens", *Soil. Found.*, **31**(1), 60-72.
Seah, T.H. and Lai, K.C. (2003), "Strength and deformation behavior of Soft Bangkok Clay", *Geotech. Test. J. ASTM*, **26**(4), 421-431.
Shibuya, S., Tamrakar, S.B. and Theramast, N. (2001), "Geotechnical site characterization on engineering properties of Bangkok Clay", *Geotech. Eng. SEAGS*, 32(3), 139-151.
Wijewickreme, D. and Vaid, Y.P. (1991), "Stress non-uniformities in hollow cylinder torsional specimens", *Geotech. Test. J. ASTM*, **14**(4), 349-362.
Yimsiri, S. and Soga, K. (2011), "Cross-anisotropic elastic parameters of two natural stiff clays", *Géotech.*, **61**(9), 809-814.
Yimsiri, S., Ratananikom, W. and Likitlersuang, S. (2009), "Investigation of some anisotropic characteristics of Bangkok Clay", *The 17th International Conference on Soil Mechanics and Geotechnical Engineering*, *17ICSMGE*, Alexandria, Egypt, 1068-1071.
Zdravkovic, L. and Jardine, R.J. (1997), "Some anisotropic stiffness characteristics of a silt under general stress conditions", *Geotech.*, 47(3), 407-437.
Zdravkovic, L. and Jardine, R.J. (2000), "Undrained anisotropy of K_o-consolidated silt", *Can. Geotech. J.*, 37(1), 178-200.
Zdravkovic, L. and Jardine, R.J. (2001), "The effect on anisotropy of rotating the principal stress axes during consolidation", *Geotech.*, **51**(1), 69-83.

CC

Notation

The following symbols are used in this paper:

b	intermediate principal stress parameter
E_u	undrained Young's modulus
E_z	undrained Young's modulus in vertical direction
E_r, E_θ	undrained Young's modulus in horizontal direction
G_{oct}	octahedral shear stiffness
$G_{z\theta}$	shear modulus in vertical plane
LL, PL, PI	liquid limit, plastic limit, and plasticity index
M_T	Torque
M, M_f	stress ratio
OCR	overconsolidation ratio
p_i	inner cell pressure
p_o	outer cell pressure
p'	mean normal effective stress
p_o'	in-situ mean normal effective stress
q	deviatoric stress
s_u	undrained shear strength
W	axial force
w_n	natural water content
Δu, Δu_f	excess pore pressure
α	major principal stress direction
α, $\alpha_{\sigma \cdot}$	major principal stress and major principal stress increment directions
α_ε, $\alpha_{\varepsilon \cdot}$	major principal strain and major principal strain increment directions
γ	total unit weight
ε_q	deviatoric strain
ε_1, ε_2, ε_3	major, intermediate and minor principal strains
ε_z, ε_r, ε_θ, $\gamma_{z\theta}$	axial, radial, circumferential and shear strains
σ_1, σ_2, σ_3	major, intermediate and minor principal stresses
σ_x, σ_y, σ_z	normal stress in x-, y-, and z-directions
σ_z, σ_r, σ_θ, $\tau_{z\theta}$	axial, radial, circumferential and shear stresses
ν_{zr}, ν_{rz}	Poisson's ratio for radial strain due to vertical direct strain and vice versa
$\nu_{z\theta}$, $\nu_{\theta z}$	Poisson's ratio for circumferential strain due to vertical strain and vice versa
$\nu_{r\theta}$, $\nu_{\theta r}$	Poisson's ratio for circumferential strain due to radial strain and vice versa
$d(\sigma_1'/\sigma_3')/dt$	principal stress increasing rate
ϕ, ϕ'_f	friction angle